Photoemission spectra and band structures of d-band metals. I. Practical aspects of fcc interpolation schemes

Neville V. Smith and L. F. Mattheiss
Bell Laboratories, Murray Hill, New Jersey 07974
(Received 21 May 1973)

A variant is described of the combined interpolation scheme for the band structures of the face-centered-cubic d-band metals, devised originally by Hodges *et al.* and by Mueller. Since it is intended to use the scheme in the interpretation of photoemission experiments, where optical transitions can occur to states well above the Fermi level, special attention has been paid to obtaining a good reproduction of the unoccupied bands. It is found that this is achieved by a suitable choice for the parameters, V_{111} and V_{200}, representing the purely local part of the pseudopotential and the coefficient S of a nonlocal contribution to the pseudopotential arising from explicit orthogonalization to the d states. The band structures of Ni, Cu, Rh, Pd, Ag, Ir, Pt, and Au have been calculated by a nonrelativistic augmented-plane-wave method, and the parameters of the scheme have been fitted to the results by a nonlinear least-squares method. These parameters are to be used in a subsequent paper as the starting point of an interpretation of photoelectron energy spectra.

I. INTRODUCTION

This is the first in a series of papers dealing with the photoemission properties of d-band metals and their interpretation in terms of one-electron band theory. Following previous work,[1,2] the aim has been to interpret photoelectron energy spectra using combined interpolation schemes. At the start of this program, two practical schemes were available, one proposed by Hodges, Ehrenreich, and Lang[3] (HEL) and the other by Mueller.[4] During the course of the work, we have developed several refinements to these original methods. These experiences are summarized in the present paper. The actual comparison between these model band structures and the experimental photoemission spectra will be made in subsequent papers. We consider here only the face-centered-cubic (fcc) d-band metals. The extension of these methods to the body-centered-cubic metals will be treated separately.

In this investigation, we have paid particular attention to the behavior of the unoccupied bands. In photoemission, one is often concerned with optical transitions to states well above the Fermi level. For example, in a conventional ultraviolet experiment where the upper limit on the photon energy is determined by the transmission cutoff of LiF windows, electrons are excited to states as high as 11.7 eV above the Fermi level. We would like to have, therefore, an accurate representation of the band structure both in this energy range and in the occupied region. Thus far, most applications of the combined interpolation schemes have concentrated on the problem of predicting Fermi-surface topologies and features of the d bands. Relatively little attention has been given to the unoccupied bands. Indeed, one finds that some of these model band structures go badly astray at higher energies. However, since the available schemes contain a large number of disposable parameters, we have investigated whether some of this flexibility can be mobilized towards the task of improving the representation of these upper bands. We find that this can indeed be done, without seriously sacrificing the accuracy of the fit to the occupied bands.

The organization of this paper is as follows: In Sec. II, we describe in some detail the derivation of the parametrized Hamiltonian of the combined interpolation scheme. The physics here is not new and is already contained in the original papers by HEL[3] and Mueller.[4] However, since we have made several modifications which may be of use to other workers, we will spell out the details of this modified scheme. In Sec. III, we describe a quick recipe for obtaining an approximate fit to the results of first-principles band calculations using this modified scheme. In particular, we discuss the relative magnitudes of the local pseudopotential and orthogonality terms which best reproduce the upper bands. Finally, in Sec. IV we present the results of a more elaborate fitting procedure which is applied to nonrelativistic first-principles augmented-plane-wave (APW) calculations for Ni, Cu, Rh, Pd, Ag, Ir, Pt, and Au.

II. PARAMETRIZED HAMILTONIAN

A. Preamble

We start with the customary 9×9 form for the model Hamiltonian

$$H=\begin{bmatrix} H_{cc} & H_{cd} \\ H_{dc} & H_{dd} \end{bmatrix} . \tag{1}$$

H_{dd} is a 5×5 block involving d-type tight-binding Bloch sums of the form

$$|d_n\rangle = N^{-1/2}\sum_l e^{i\vec{k}\cdot\vec{R}_l}\,\psi_n(\vec{r}-\vec{R}_l) . \tag{2}$$

N is the number of atoms in the crystal and $\vec{R}_l$ is the position vector for the atom at site l. The atomic d orbitals $\psi_n(\vec{r})$ are chosen to be of the form

$$\begin{aligned} &\psi_1 = xyf(r)/r^2, \quad \psi_2 = yzf(r)/r^2, \\ &\psi_3 = zxf(r)/r^2, \quad \psi_4 = \tfrac{1}{2}(x^2-y^2)f(r)/r^2, \\ &\psi_5 = \tfrac{1}{6}\sqrt{3}\,(3z^2-r^2)f(r)/r^2. \end{aligned} \tag{3}$$

H_{cc} is a 4×4 plane-wave block and H_{cd} is a 5×4 hybridization block. Here we work in the same $\frac{1}{48}$th irreducible wedge of the Brillouin zone used by HEL[3] (namely, $k_y \geq k_x \geq k_z$). The appropriate set of normalized plane waves, $|k_i\rangle$, for reduced wave vectors $\vec{k}$ within this wedge involves the following wave vectors:

$$\begin{aligned} &\vec{k}_1 = \vec{k}, \quad \vec{k}_2 = \vec{k} + (2\pi/a')\,(0,-2,0), \\ &\vec{k}_3 = \vec{k} + (2\pi/a')\,(-1,-1,-1), \\ &\vec{k}_4 = \vec{k} + (2\pi/a')(-1,-1,1). \end{aligned} \tag{4}$$

With these nine basis states, the aim is to set up a model Hamiltonian whose matrix elements have the simplest possible form, yet whose eigenvalues reproduce those obtained in first-principles band calculations. In doing this, one encounters hybridization and overlap integrals of the type $\langle d_n|H|\vec{k}_i\rangle$ and $\langle d_n|\vec{k}_i\rangle$. Whenever these occur, our procedure (which follows closely but not precisely that established by HEL[3] and Mueller[4]) is to introduce the following parametrized forms:

$$\langle d_n|\vec{k}_i\rangle = af(k)\,Y_{2n}(\vec{k}_i), \tag{5}$$

$$\langle d_n|H|\vec{k}_i\rangle = bg(k)\,Y_{2n}(\vec{k}_i) . \tag{6}$$

The coefficients a and b are treated as disposable parameters and the functions $Y_{2n}(\vec{k}_i)$ represent the set of real spherical harmonics given by

$$\begin{aligned} &Y_{21}(\vec{q}) = q_xq_y/q^2, \quad Y_{22}(\vec{q}) = q_yq_z/q^2, \\ &Y_{23}(\vec{q}) = q_zq_x/q^2, \quad Y_{24}(\vec{q}) = \tfrac{1}{2}(q_x^2-q_y^2)/q^2, \\ &Y_{25}(\vec{q}) = \tfrac{1}{6}\sqrt{3}\,(3q_z^2-q^2)/q^2, \end{aligned} \tag{7}$$

where n corresponds to the subscripts in Eq. (3). These spherical harmonics obey the addition theorem

$$\sum_n Y_{2n}(\vec{q})\,Y_{2n}(\vec{q}') = \tfrac{1}{5}P_2(\hat{q}\cdot\hat{q}'), \tag{8}$$

where $P_2(x) = \frac{1}{2}(3x^2-1)$ is the usual $l=2$ Legendre polynomial, $\hat{q}$ and $\hat{q}'$ are unit vectors, and x is the cosine of the angle between $\vec{q}$ and $\vec{q}'$.

The functions $f(k)$ and $g(k)$ are radial form factors which we parametrize as

$$f(k) = g(k) = j_2(kR), \tag{9}$$

where R is a parameter and j_2 is the usual spherical Bessel function of the order 2. Note that we have used the same functional form for both $f(k)$ and $g(k)$. This is useful though not an essential assumption. In fact, Mueller[4] employs the spherical-Bessel-function form for both $f(k)$ and $g(k)$ but introduces two separate radii, R_0 and R_1. However, using the same arguments for both the hybridization and overlap parameters leads to simplifications in the algebra, as will be shown below.

B. d-d block, H_{dd}

The standard procedure is to express the elements of this block, $\langle d_n|H|d_m\rangle$, in the tight-binding form given by Slater and Koster[5] or Fletcher and Wohlfarth.[6] For the most part, we have used the nearest-neighbor three-center form, as worked out by Fletcher.[7] An alternative two-center form, extended to second-nearest neighbors, is considered in Sec. IV. The Fletcher notation involves eight parameters: E_0, Δ, A_1, A_2, A_3, A_4, A_5, and A_6. The last six specify the dispersion of the bands while E_0 and $E_0+\Delta$ are the mean energies of the t_{2g} and e_g subbands, respectively.

C. Hybridization block, H_{cd}

Following Mueller,[4] we orthogonalize the plane waves to the d states explicitly. The set of orthogonalized plane waves (OPW's) is given by

$$|\phi_i\rangle = c_i^{-1}\left(|\vec{k}_i\rangle - \sum_n |d_n\rangle\langle d_n|\vec{k}_i\rangle\right), \tag{10}$$

where

$$c_i = \left(1-\sum_n |\langle d_n|k_i\rangle|^2\right)^{1/2} . \tag{11}$$

The elements of the hybridization block are then given by

$$\langle\phi_i|H|d_n\rangle = c_i^{-1}\left(\langle\vec{k}_i|H|d_n\rangle - \sum_m \langle\vec{k}_i|d_m\rangle\langle d_m|H|d_n\rangle\right) . \tag{12}$$

This expression can be simplified if dispersion effects within the d bands are neglected and the matrix $\langle d_m|H|d_n\rangle$ is replaced by the diagonal matrix consisting of E_0 times the unit matrix. Substituting Eqs. (5), (6), and (9) into Eq. (12), we obtain

$$\begin{aligned} \langle\phi_i|H|d_n\rangle &= c_i^{-1}(b-E_0a)\,j_2(k_iR)\,Y_{2n}(\vec{k}_i) \\ &= Bj_2(k_iR)\,Y_{2n}(\vec{k}_i) . \end{aligned} \tag{13}$$

Here, we have neglected the weak k dependence of c_i and have lumped together various parameters into the new disposable parameter B. Following HEL,[3] we also reserve the possibility that B may

be different for the orbitals with t_{2g} and e_g symmetry. In this case, we write

$$B = B_t \text{ for } n = 1, 2, \text{ or } 3,$$
$$B = B_e \text{ for } n = 4 \text{ or } 5. \tag{14}$$

D. Plane-wave block, H_{cc}

Since we are ultimately concerned with the solution of a secular equation of the type $\det||H-E||=0$ we consider the matrix elements of $H-E$ rather than H. This is not necessary in the hybridization and d-d blocks because the d states $|d_n\rangle$ are assumed to be mutually orthogonal and the OPW's have been explicitly orthogonalized to them. The matrix elements of the plane-wave block are given by

$$\begin{aligned}\langle\phi_i|(H-E)|\phi_j\rangle = c_i^{-1}c_j^{-1}\Big(&\langle\vec{k}_i|H|\vec{k}_j\rangle \\ &-\sum_n \langle\vec{k}_i|d_n\rangle\langle d_n|H|\vec{k}_j\rangle \\ &-\sum_n \langle\vec{k}_i|H|d_n\rangle\langle d_n|\vec{k}_j\rangle \\ &+\sum_{n,m} \langle\vec{k}_i|d_n\rangle\langle d_n|H|d_m\rangle\langle d_m|\vec{k}_j\rangle - E\delta_{ij} \\ &+E\sum_n \langle\vec{k}_i|d_n\rangle\langle d_n|\vec{k}_j\rangle\Big).\end{aligned} \tag{15}$$

The first term in the parentheses is written in the standard nearly-free-electron (NFE) form

$$\langle\vec{k}_i|H|\vec{k}_j\rangle = \alpha k_i^2\delta_{ij} + V_{ij}. \tag{16}$$

The free-electron value of α would be $(\hbar^2/2m)\times(\pi/4a')^2$ where a' is the lattice constant. The V_{ij} are pseudopotential coefficients, of which only the lowest three (V_{000}, V_{111}, and V_{200}) are assumed to be nonzero. Other terms within the parentheses are simplified as follows. In the double sum over n and m, we once again neglect the dispersion of the d bands by setting $\langle d_n|H|d_m\rangle = E_0\delta_{nm}$. Using Eqs. (4), (5), and (7), we obtain

$$\begin{aligned}\langle\phi_i|(H-E)|\phi_j\rangle = (c_i^{-1}c_j^{-1}\alpha k_i^2 - E)\delta_{ij} + c_i^{-1}c_j^{-1}V_{ij} \\ + \tfrac{1}{3}c_i^{-1}c_j^{-1}[-2ab + a^2E_0 + a^2E(1-\delta_{ij})] \\ \times j_2(k_iR)j_2(k_jR)P_2(\hat{k}_i\cdot\hat{k}_j).\end{aligned} \tag{17}$$

Note that setting $f(k)=g(k)$ in Eq. (8) is essential to obtain the simple form of the final term in Eq. (17). We can absorb the normalization factors c_i and c_j by redefining the parameters α and V_{ij}. By neglecting the off-diagonal E dependence within the square brackets and representing the remaining terms by S, we obtain the expression

$$\langle\phi_i|(H-E)|\phi_j\rangle = \langle\phi_i|H|\phi_j\rangle - E\delta_{ij}.$$

The first term is an energy-independent Hamiltonian given by

$$\begin{aligned}\langle\phi_i|H|\phi_j\rangle = \alpha k_i^2\delta_{ij} + V_{ij} \\ + Sj_2(k_iR)j_2(k_jR)P_2(\hat{k}_i\cdot\hat{k}_j).\end{aligned} \tag{18}$$

Apart from the last term, this is the same as the plane-wave block of the HEL scheme. The H_{cd} and H_{dd} blocks of the HEL and Mueller schemes are essentially identical. What we have demonstrated, therefore, is that the essence of Mueller's orthogonalization refinement can be captured in the HEL scheme by adding to each element of the plane-wave block a single additional term. We refer to this term as the orthogonalization term or S term. We refer to the V_{ij} term as the local pseudopotential. The combination of the V_{ij} and S terms may be thought of as a nonlocal pseudopotential.

One cannot help noting a strong resemblance between the S term and the $l=2$ terms which enter the standard APW and Korringa-Kohn-Rostoker-Ziman (KKRZ)-pseudopotential methods.[8] In terms of this analogy, one would identify the parameter R as the muffin-tin radius while S would be given by an expression involving phase shifts or logarithmic derivatives. For our purposes, however, S and R are treated as disposable parameters. Because of this similarity, it is not too surprising that, through the inclusion of the S term, the present scheme is better able to mimic the detailed results of first-principles band-structure calculations.

E. Symmetrizing factors

We have shown in Sec. II D that the orthogonality effects discussed by Mueller can be incorporated into the HEL scheme by the addition of a simple new term to the HEL plane-wave block. With this addition, we will follow, hereon, the HEL scheme. In particular, we retain the so-called symmetrizing factors. The need for these arises from the fact that the four plane waves or OPW's are a truncated set and do not reflect the full symmetry of the crystal. The symmetrizing factors allow one to remedy this defect and restore the symmetry-induced degeneracies at symmetry points. According to HEL,[3] each OPW, $|\phi_i\rangle$, has associated with it a $\vec{k}$-dependent symmetrizing factor $F_i(\vec{k})$. These are equal to 1 or 0 at points of high symmetry, depending on whether or not the corresponding OPW bands are involved in the desired symmetric combination at that point. The variation between these values is arbitrary. The following form is assumed for the symmetrizing factors of the OPW's with wave vectors given by Eq. (4)[9]:

$$\begin{aligned}F_1 &= 1, \\ F_2 &= \left[\sin\left(\frac{\pi}{2}\,\frac{k_y-k_x}{16-k_x-k_y}\right)\right]^{1/2}, \\ F_3 &= \left[\sin\left(\frac{\pi}{2}\,\frac{k_x+k_z}{12-k_y}\right)\right]^{1/2},\end{aligned} \tag{19}$$

$$F_4 = \left[\sin\left(\frac{\pi}{2}\,\frac{k_x - k_z}{12 - k_y}\right)\right]^{1/2} .$$

These are introduced into the model Hamiltonian by multiplying each off-diagonal element, $\langle \phi_i | H | \phi_j \rangle$, of the plane-wave block by $F_i F_j$ and each element, $\langle \phi_i | H | d_n \rangle$, of the hybridization block by F_i. These functions in Eq. (19) differ from those used by HEL but are similar to alternatives proposed by Smith.[2] The present choice for the functional form of these symmetrizing factors is based on the results of studies that are described in Sec. III C.

To illustrate the role of these symmetrizing factors, we plot in Fig. 1 the free-electron bands involving the four OPW's with wave vectors given by Eq. (4). In this figure, the solid (dotted) lines designate bands for which the symmetrizing factors are 1 (0). In those cases where the symmetrizing factor varies from 1 to 0, the long (short) dashed lines indicate schematically those portions where the symmetrizing factor is large (small). From these results, it is clear that the symmetrizing factors play an important secondary role; namely, they eliminate the need to modify the functional form of $f(k)$ and $g(k)$ in Eq. (9) at large k. Mueller[4] introduces such a cutoff to eliminate hybridization and orthogonality corrections involving these higher OPW's.

One of the less attractive features of the present scheme is the fact that the quality of the fit depends on these rather artificial symmetrizing factors. However, there appears to be no satisfactory method for eliminating them without increasing the size of the plane-wave block of the model Hamiltonian.

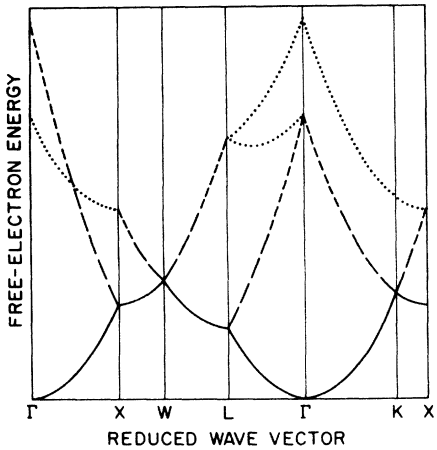

FIG. 1. Schematic representation of the strengths of the symmetrizing factors associated with the plane-wave bands. The full (dotted) curves indicated free-electron bands for which the symmetrizing factors are 1 (0). For the other bands, the symmetrizing factors vary smoothly from 1 to 0.

III. QUICK PROCEDURE FOR FITTING BANDS

The model Hamiltonian is sufficiently simple in form that, at points of high symmetry, it is easily reduced by hand. In this section, we present these results for the symmetry points Γ, X, L, and W and show how they may be used in terms of a quick "recipe" to fit the results of first-principles calculations and thereby determine the parameters of the plane-wave- and hybridization-blocks. In particular, we discuss the best choice for the magnitude of the orthogonalization term.

We assume that the parameters of the d-d block have already been found. These can be determined quickly by fitting a few of the nonhybridizing d levels. Within the context of the present scheme, the levels $\Gamma_{25'}$, Γ_{12}, X_5, X_3, X_2, L_3^u, L_3^l, and K_4 are pure d states and these may be used to determine the d band parameters. In the case of Burdick's APW results on Cu,[10] which we will take as our example in what follows, the values found in this way[11] for the parameters E_0, Δ, A_1, A_2, A_3, A_4, A_5, and A_6 are given in column (a) of Table I.

When hybridization is introduced (i.e., $B \neq 0$), it is found that the energies of several pairs of states at X, L, and W are given by a simple quadratic equation of the form[11]

$$(E - E_d)(E - E_c) = \gamma^2, \tag{20}$$

where E_d and E_c are the d band and OPW energies, respectively, when $B_t = B_e = 0$. We now summarize these results. We introduce the abbreviations j_L j_X, and j_W to denote the values of $j_2(kR)$ at L, X, and W, respectively.

A. Energy eigenvalues at L, X, and W

At L, we have $F_1 = 1$, $F_2 = 0$, $F_3 = 1$, and $F_4 = 0$. The sum and difference of $|\phi_1\rangle$ and $|\phi_3\rangle$ yields functions which transform like L_1 and $L_{2'}$, respectively. In the absence of hybridization, we obtain the following NFE form for the energies E_c:

$$E_c(L_1) = T(L) + V'_{111}(L), \tag{21}$$

$$E_c(L_{2'}) = T(L) - V'_{111}(L), \tag{22}$$

where the kinetic energy term $T(L)$ and the nonlocal pseudopotential term $V'_{111}(L)$ are given by[9]

$$T(L) = 48\alpha + V_{000} + Sj_L^2 , \tag{23}$$

$$V'_{111}(L) = V_{111} + Sj_L^2 . \tag{24}$$

Note that the $E(L_{2'})$ is independent of the S-term whereas $E(L_1)$ includes a contribution $2Sj_L^2$. The contribution of this nonsymmetric orthogonality term to the $L_1 - L_{2'}$ splitting has been discussed previously by Mueller.[4] In addition to these effects, the L_1 level also hybridizes with a d level of the

TABLE I. Interpolation scheme parameters for Burdick's *APW* results on Cu, from (a) quick fitting procedure and (b) nonlinear least-squares fitting.

	a	b
α	0.01397	0.01401
V_{000}	−0.1000	−0.1119
V_{111}	0.0553	0.0529
V_{200}	0.0773	0.0761
R	0.40	0.4111
S	0.866	0.7341
B_t	0.970	1.0562
B_e	0.970	1.0818
E_0	0.33075	0.32818
A_1	0.02031	0.02038
A_2	0.00619	0.00556
A_3	0.01025	0.00754
A_4	0.01295	0.01094
A_5	0.00262	0.00287
A_6	0.00826	0.00931
Δ	−0.00445	0.00244

same symmetry; as a result, Eq. (20) applies with

$$E_d(L_1) = E_0 - 8A_3, \tag{25}$$

$$\gamma(L_1) = (\sqrt{\tfrac{2}{3}})B_t j_L\ . \tag{26}$$

At X, we have $F_1 = F_2 = 1$ and $F_3 = F_4 = 0$. The situation is similar to that at L, in that the remaining two OPW's form symmetric and antisymmetric combinations which transform as X_1 and $X_{4'}$, respectively. In this case,

$$E_c(X_1) = T(X) + V'_{200}(X), \tag{27}$$

$$E_c(X_{4'}) = T(X) - V'_{200}(X), \tag{28}$$

where

$$T(X) = 64\alpha + V_{000} + Sj_X^2, \tag{29}$$

$$V'_{200}(X) = V_{200} + Sj_X^2\ . \tag{30}$$

The X_1 level also hybridizes with a d level and

$$E_d(X_1) = E_0 + \Delta - \tfrac{20}{3}A_4 - \tfrac{8}{3}A_5, \tag{31}$$

$$\gamma(X_1) = -(\sqrt{\tfrac{2}{3}})B_e j_X\ . \tag{32}$$

At W, $F_i = 1$ for $i = 1$ to 4 so that we must contend simultaneously with all four OPW's. In the absence of hybridization, symmetrized combinations of these OPW's yield two singly-degenerate levels W_1 and $W_{2'}$ and a doubly-degenerate W_3 level, with

$$E_c(W_1) = T(W) + 2V'_{111}(W) + V'_{200}(W), \tag{33}$$

$$E_c(W_{2'}) = T(W) - 2V'_{111}(W) + V'_{200}(W), \tag{34}$$

$$E_c(W_3) = T(W) - V'_{200}(W) \tag{35}$$

and

$$T(W) = 80\alpha + V_{000} + Sj_W^2, \tag{36}$$

$$V'_{111}(W) = V_{111} - \tfrac{11}{25}Sj_W^2, \tag{37}$$

$$V'_{200}(W) = V_{200} + \tfrac{1}{25}Sj_W^2\ . \tag{38}$$

Each of these states hybridizes with a d level according to Eq. (20), with

$$E_d(W_1) = E_0 + \Delta + \tfrac{4}{3}A_4 + \tfrac{16}{3}A_5, \tag{39}$$

$$E_d(W_{2'}) = E_0 + \Delta - 4A_4, \tag{40}$$

$$E_d(W_3) = E_0 - 4A_2 \tag{41}$$

and

$$\gamma(W_1) = -\tfrac{2}{15}\sqrt{3}\,B_e j_W\ , \tag{42}$$

$$\gamma(W_{2'}) = -\tfrac{4}{5}B_e j_W, \tag{43}$$

$$\gamma(W_3) = +\tfrac{2}{5}\sqrt{2}\,B_t j_W \tag{44}$$

B. Recipe for fitting

Since we assume that the d-band parameters have already been found, we can calculate E_d for each of the pairs of hybridizing levels discussed above. The two eigenvalues (E_u and E_l) which we wish to fit with Eq. (20) are also known (they may be read off from the same first-principles $E(\vec{k})$ curves that were used previously to deduce the d-band parameters). According to the diagonal-sum rule, $E_u + E_l = E_d + E_c$, so that

$$E_c = E_u + E_l - E_d, \tag{45}$$

setting $E = E_u$ in Eq. (20) and eliminating E_c with Eq. (45), we find

$$\gamma^2 = (E_u - E_d)(E_d - E_l)\ . \tag{46}$$

Using Eqs. (45) and (46), we can calculate E_c and γ for each pair of hybridized levels. Each value for γ yields a corresponding value of $Bj_2(kR)$. From these results, one may choose the optimum values for the parameters B and R. In the present example (Burdick's APW calculation for Cu[10]), the values $B = 0.970$ Ry and $R = 0.400$ are obtained. In this simplified method, we ignored the value of Bj_W obtained for W_1 since it differs widely from the values of Bj_W obtained from the $W_{2'}$ and W_3 states. In absolute terms, the actual hybridization shift is small for W_1, and therefore susceptible to a large percentage error. As a result, it is advantageous to use only the larger shifts associated with $W_{2'}$ and W_3.

Having determined R, this fixes the values of j_X, j_L, and j_W. Let us turn now to the values obtained for E_c and show how they lead to estimates for V_{111}, V_{200}, and S. We will require the values of $E_c(L_{2'})$ and $E_c(X_{4'})$. Since these levels do not hybridize, their energies may be read off directly from the results of a first-principles calculation. Applying the appropriate equations of Sec. III A to Burdick's Cu results,[10] we find

$$
\begin{aligned}
V'_{111}(L) &= V_{111} + S j_L^2 \\
&= \tfrac{1}{2}[E_c(L_1) - E_c(L_{2'})] = 0.1251 \quad \text{Ry}, \\
V'_{200}(X) &= V_{200} + S j_X^2 \\
&= \tfrac{1}{2}[E_c(X_1) - E_c(X_{4'})] = 0.1585 \quad \text{Ry}, \\
V'_{111}(W) &= V_{111} - \tfrac{11}{25} S j_W^2 \\
&= \tfrac{1}{4}[E_c(W_1) - E_c(W_{2'})] = 0.0207 \quad \text{Ry}, \\
V'_{200}(W) &= V_{200} + \tfrac{1}{25} S j_W^2 \\
&= \tfrac{1}{4}[E_c(W_1) + E_c(W_{2'}) - 2E_c(W_3)] \\
&= 0.0848 \quad \text{Ry}.
\end{aligned}
\tag{47}
$$

We therefore have four equations with three unknowns, V_{111}, V_{200}, and S. Happily, a reasonable solution is possible for Cu with $V_{111} = 0.0553$ Ry, $V_{200} = 0.0773$ Ry, and $S = 0.866$ Ry, respectively.

All that remains is the determination of the final two parameters, V_{000} and α. The first is readily evaluated since $E(\Gamma_1) = V_{000}$. The second is determined by noting that the values of $T(L)$, $T(X)$, and $T(W)$ can be obtained from the previously determined values of E_c. Using Eqs. (23), (29), and (36), we obtain three estimates for α. In the case of Cu, the average of these gives $\alpha = 0.013\,97$.

The values of the parameters obtained in this way for Cu are shown in column (a) of Table I. Column (b) shows the values obtained by a more elaborate nonlinear least-squares fitting procedure described in Sec. IV of this paper. It is seen that the recipe described here gives values not far different from those obtained via the more elaborate procedure.

In Fig. 2 we show the bands obtained using the parameter set of column (a) of Table I. The results are compared with the actual APW eigenvalues of Burdick indicated by filled circles. The open circles represent the levels used in the quick fitting recipe to determine the parameters of the plane-wave and hybridization blocks. It is seen that the fit is quite close. The fit to the d bands is comparable to that obtained by HEL and Mueller. We draw particular attention, however, to the quality of fit in the unoccupied region. The fit is quite good up to about 1.4 Ry (i.e., about 11 eV above the Fermi level) which is quite adequate for analysis of conventional photoemission experiments. Above this value, the bands begin to go astray. The eighth and ninth bands at X, for example, (which transform as $X_{5'}$) are in error by more than 2 eV.

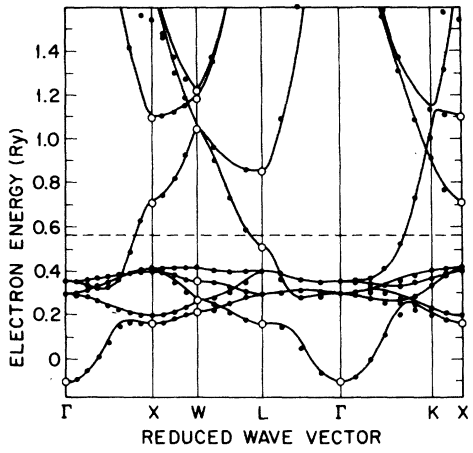

FIG. 2. Energy-band results for Cu that are generated by the parameters in column (a) of Table I. The filled circles represent Burdick's APW eigenvalues. The open circles represent those eigenvalues that are involved in the fitting procedure of Sec. III.

C. Relative magnitudes of orthogonalization and pseudopotential terms

There has been some discussion in the literature[4,12] concerning the relative contributions of the local pseudopotential (V_{111}) and the orthogonalization term (S term) to the L_1-$L_{2'}$ splitting. We refer here only to the difference between $E_c(L_1)$ and $E_c(L_{2'})$ when hybridization with the d bands is neglected. Hybridization can increase (decrease) this gap if the L_1 state is above (below) $L_{2'}$. In the original HEL scheme where there is no S term, the L_1-$L_{2'}$ splitting is due entirely to V_{111}. In Mueller's original parameterization, V_{111} and V_{200} are assumed to be small in analogy with the situation in Al so that his orthogonality terms provides the main contribution to this gap. While both parameterizations yield the correct $L_{2'} - L_1$ separation, as well as a reasonable $X_{4'} - X_1$ gap, they go badly astray at other points in the zone. In particular, the band gaps at W are not well reproduced. In the present parametrization scheme, we have emphasized the importance of fitting that bands at W. It has been found that, in order to do this, the magnitudes of V_{111} and the S term must be roughly comparable. The present scheme is therefore a compromise between the two extremes represented in the HEL and Mueller schemes.

The comparison between the various parametrizations is illustrated in Fig. 3, where we show the band structure of Cu in the $X \rightarrow W$ and $W \rightarrow L$ directions. The middle panel, Fig. 3(b), represents the same parametrization given in Table I, column (a), illustrated in Fig. 2. Figures 3(a) and 3(c) represent simulations of the HEL and Mueller parametrizations. These were obtained by varying α, V_{111}, V_{200}, and S, but in such a way as to leave the energies of the levels $L_{2'}$, L_1, and $X_{4'}$ unaffected. All other parameters of the scheme are kept constant. The HEL scheme is retrieved

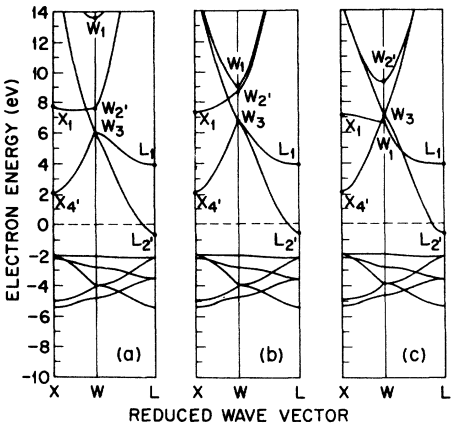

FIG. 3. Comparison of three alternative parametrizations: (a) the original HEL parametrization (zero S-term); (b) the present parametrization; (c) a simulation of Mueller's parametrization (large-S term and small V_{111}, V_{200}).

simply by setting S equal to zero. The Mueller parametrization is *simulated* (because of the simplification introduced in Sec. II, there are some minor differences with the actual Mueller scheme) by setting α equal to its free-electron value. One finds that this forces V_{111} and V_{200} to be small and the S term to be rather large.

It can be seen in Fig. 3 that the level most affected by these changes is the s-like level W_1. In the HEL parametrization scheme, this level occurs several electron volts higher than it should. Why this happens is immediately obvious from Eqs. (33)–(38). If S is zero and V_{111} and V_{200} are large and positive, then $E_c(W_1)$ is forced upwards. This gross error in the positioning of W_1 (and the rest of the ninth band) is present in previous calculations of the joint density of states and the energy distribution of the joint density of states.[1,2] Its most serious effect is that in describing optical transitions from, say, the d bands to the ninth band, the calculations overestimate the threshold for optical transitions near W, raising it above the normal upper limit of the calculations (12 eV).

An important goal of the present parametrization scheme is to reproduce the correct band gaps at W. This is achieved by the S term in the following way. Since both V_{111} and S are positive, the V_{111} and the S terms at the L point in the Brillouin zone reinforce each other to give a large value of the nonlocal pseudopotential V'_{111}. At W, however, the behavior of the Legendre polynomial P_2 causes the S term to reverse its sign and, according to Eq. (36), this cancels most of V_{111} and yields a much smaller V'_{111}. In a similar way, V'_{200} is reduced by a factor of 2 in going from X to W. These changes are in the correct sense and of the correct relative magnitude to reproduce the results of first-principles band calculations. Mueller's parametrization tends to "overdo" the variation of V'_{111} and V'_{200} with $\vec{k}$. If the S term dominates, it can be seen from Eq. (36) that V'_{111} will swing negative at W, thus inverting the order of the $W_{2'}$ and W_1 levels. This in turn causes crossings between the bands joining $L_{2'}$ to W_3 and L_1 to W_1.

D. Simulation of relativistic effects

Relativistic effects in the $5d$ transition metals, and even the $4d$ series, are quite large. It is therefore desirable to make some provision for including them in the scheme. The most important relativistic effect is the spin-orbit coupling since it lifts degeneracies and brings about a qualitative change in the nature of the bands. When spin-orbit coupling is included, the model Hamiltonian of Eq. (1) is applied to both the spin-up and spin-down electrons. The total Hamiltonian has the form

$$H_{\mathrm{rel}}=\begin{bmatrix} H_{cc} & H_{cd} & 0 & 0 \\ H_{dc} & H_{dd}+\xi M & 0 & \xi N \\ 0 & 0 & H_{cc} & H_{cd} \\ 0 & -\xi N^{*} & H_{dc} & H_{dd}+\xi M^{*} \end{bmatrix}, \tag{48}$$

where M and N, which involve a single additional parameter ξ, are given by Friedel *et al.* and Abate and Asdente.[13] For simplicity, one can set the spin-orbit parameter ξ equal to the corresponding atomic value from Herman and Skillman[14] and thereby avoid the introduction of yet another parameter.

The influence of the other relativistic effects (mass-velocity and Darwin terms) can be absorbed by readjusting parameters in the original nonrelativistic scheme. We have found that the special properties of the S term can be exploited to good advantage here. Let us consider the case of Au, where Christensen and Seraphin[15] have published eigenvalues for relativistic and nonrelativistic APW calculations. We consider the plane-wave gaps at L and X. In the double-group notation of the Christensen-Seraphin paper, the relativistic L_{4^+} and L_{4^-} states correspond to the nonrelativistic L_1 and $L_{2'}$ levels, respectively. Similarly, the levels X_{6^+} and X_{6^-} correspond to X_1 and $X_{4'}$, respectively. Comparing the relativistic and nonrelativistic eigenvalues, we find that the combined effect of the mass-velocity and Darwin terms is to lower both the p-like $L_{2'}$ and $X_{4'}$ levels by 0.12 and 0.16 Ry, respectively. Likewise, the s-like levels L_1 and X_1 are depressed by 0.35 and 0.38 Ry, respectively. These results are consistent with the relativistic shifts of the $6p$ and $6s$ states of the free atom, as given by Herman and Skillman.[14] We

note, in particular, that the downward shift of the s-like levels is greater than that of the p-like levels. This results in narrower band gaps at both X and L.

Let us consider how these results can resolve the ambiguities that arise in the corresponding states at W. In the nonrelativistic limit, there are four levels: the s-type W_1, the p-type $W_{2'}$, and the doubly degenerate p-type W_3 levels. In the relativistic limit, one has four singly degenerate levels (W_6, W_7, W_6 and W_7). The relationship between the relativistic and nonrelativistic levels is, at first sight, ambiguous. In general, one would like to know the ordering of the W_1, $W_{2'}$, and W_3 levels if spin-orbit coupling were neglected in the relativistic calculations but the other relativistic effects were retained. The best way to answer this question is to perform the relativistic-rAPW calculations with spin-orbit coupling included and then omitted. Short of this, we can proceed approximately as follows. We apply to the nonrelativistic s- and p-like levels at W the same shifts found for the s- and p-like levels at L and X, respectively. This leaves the relative separation between the p-like levels $W_{2'}$ and W_3 unchanged. However, owing to the greater downward shift for the s-like levels, the W_1 level (which lies close to $W_{2'}$ in the nonrelativistic case) should be the lowest state in the relativistic limit. In Christensen and Seraphin's Au calculation, we identify the lowest relativistic-plane-wave W_6 state with W_1, and the uppermost W_7 level with $W_{2'}$. The average of the two intermediate W_6 and W_7 levels then corresponds to the doubly degenerate W_3 state.

The shifts described above are very readily accommodated by adjustments to the parameters of the nonrelativistic scheme. The narrowing of the gaps at X and L is readily simulated by adjusting V_{111}, V_{200}, and S (and possibly α). This is done in such a way that, although the magnitude of the band gaps decrease, the contribution of the S term increases relative to V_{111} and V_{200}. Ultimately, this causes V'_{111} to change sign at W, thereby inverting W_1 and $W_{2'}$. We recall that this is precisely the ordering that occurs in the Mueller scheme, where V_{111} and V_{200} are constrained to be small.

IV. NONLINEAR LEAST-SQUARES FIT TO APW RESULTS

A series of nonrelativistic APW calculations have been performed for the fcc metals in the $3d$ (Ni, Cu), $4d$ (Rh, Pd, Ag), and $5d$ (Ir, Pt, Au) transition series. The purpose of these calculations is to provide a first-principles estimate of the interpolation parameters for each of these metals. It is anticipated that these results will serve as a useful starting point for subsequent attempts to fit the observed structure in the photoelectron energy spectra for these materials. Since the present APW calculations neglect relativistic effects, such an empirical-adjustment procedure will have to make corrections for these errors as well as those introduced as a result of inaccuracies in the crystal potential.

A. Details of APW calculation

The present APW calculations for these fcc metals involve approximate crystal potentials that are derived from the atomic charge densities of Herman and Skillman.[14] Exchange and correlation effects are included by means of Slater's original $\rho^{1/3}$ approximation.[16]

These calculations improve the muffin-tin approximation to the crystal potential by including corrections to the constant potential outside the APW spheres. The techniques for calculating the muffin-tin potentials and the corrections have been described previously.[17] In the present close-packed fcc structure, these corrections to the muffin-tin potential are expected to have a small effect on the energy eigenvalues. Prior studies by Koelling, *et al.*[18] for Pd and Pt indicate that these corrections shift energy eigenvalues by 0.001–0.005 Ry, and in a few cases by 0.010–0.015 Ry.

We list in Table II the atomic configurations and the lattice constants that are involved in determination of the individual crystal potentials. In each case, the APW sphere radii were chosen so that neighboring spheres touched along the ⟨110⟩ directions. The atomic configurations for Rh, Pd, Ir, and Pt are identical with those used in previous calculations by Andersen.[19]

B. Determination of parameters

The APW calculations for each metal were carried out at seven points of high symmetry in the fcc Brillouin zone, including $\Gamma(0, 0, 0)$, $X(0, 8, 0)$, $L(4, 4, 4)$, $W(4, 8, 0)$, $K(6, 6, 0)$, $\Delta(0, 4, 0)$, and $\Sigma(4, 4, 0)$. The model Hamiltonian parameters were determined by applying a nonlinear least-squares procedure[20] to fit the energy eigenvalues of the 40 states listed in Table III. This fit did not involve some of the higher-energy OPW states (Δ_1, Σ_1, and Σ_3) that are generated by the model Hamiltonian. In the fitting procedure, each eigenvalue is given equal weight, regardless of its degeneracy or location in the Brillouin zone.

For purposes of comparison, we first applied this fitting procedure to the results of Burdick's APW calculation for Cu. The resulting set of parameters is listed in column (b) of Table I. Encouragingly, the values for these parameters are in good agreement with those obtained by the less elaborate recipe of Sec. III.

TABLE II. Atomic configurations and lattice constants for the fcc metals.

Element	Ni	Cu	Rh	Pd	Ag	Ir	Pt	Au
Atomic no.	28	29	45	46	47	76	77	78
Configuration	$3d^8 4s^2$	$3d^{10} 4s^1$	$4d^8 5s^1$	$4d^{10}$	$4d^{10} 5s^1$	$5d^7 6s^2$	$5d^9 6s^1$	$5d^{10} 6s^1$
Lattice constant Å	3.5166[a]	3.6147[b]	3.8031[c]	3.8898[c]	4.0855[b]	3.8389[c]	3.2931[c]	4.0781[b]
Muffin-tin V_0 (Ry)	−1.392	−1.078	−1.249	−0.848	−0.932	−1.500	−1.179	−1.012

[a]E. I. Zornberg, Phys. Rev. B 1, 244 (1970).
[b]W. J. O'Sullivan, A. C. Switendick, and J. E. Schirber, Phys. Rev. B 1, 1443 (1970).
[c]O. K. Andersen, Phys. Rev. B 2, 883 (1970).

The corresponding parameters that are obtained from a similar fit to the present APW results are listed in Table IV. In each case, the rms and maximum errors involved in the fit are listed. These errors, which are roughly proportional to the bandwidths, are largest in the case of Ir. It is found that the parameter A_1 provides a useful estimate of the d bandwidth since its magnitude is consistently about 10% of the total d bandwidth. It should be emphasized that no attempt has been made, at this stage, to bring these band structures into agreement with any experimental data. The model band structures obtained using these parameters are illustrated for the ΓX direction in Fig. 4.

C. Improvements

We have investigated several possible means for improving the accuracy of the present model Hamiltonian. In one such study, we reduced the six three-center nearest-neighbor d-d parameters A_1–A_6 to three parameters via the two-center approximation and then added second-neighbor interactions. The corresponding parameters for this case are included in Table V. A comparison between the results of Tables IV and V indicates that both variations reproduce the APW results with comparable accuracy.

We have also studied the relationship between accuracy and the functional form of the symmetrizing factors F_1 in Eq. (19). In the present fitting procedure, these are particularly important at the Σ and Δ points in the Brillouin zone where the symmetrizing factors assume value intermediate between 0 and 1 (see Appendix). The results of these studies indicate that the $\sin^{1/2}x$ form of Eq. (19) provides a more accurate fit than the previously suggested $\sin^2 x$ dependence.[2]

Other possible sources of error include the approximations introduced in Secs. II C and II D, where the effects of d-band dispersion were neglected in parametrizing various hybridization and orthogonality terms in the model Hamiltonian. We recall that $\vec{k}$-dependent normalization factors were absorbed into the parameters α, V_{111}, V_{200}, V_{000}, and S, and thereafter, these were treated as constants. We have tested the accuracy of these approximations by introducing overlap between the OPW and d-type states explicitly in the matrix elements of $H-E$. Equations (5) and (6) were used to parametrize the overlap and hybridization matrix elements, respectively. For maximum flexibility, two separate radii were introduced so that $f(k)=j_2(kR_0)$ and $g(k)=j_2(kR_1)$. The results of the corresponding nonlinear least-squares fit reduced the rms error by about 20%. However, part of this improvement can be attributed to the two additional parameters that were introduced. We conclude that the approximations of Secs. II C and II D are reasonably accurate.

It appears that the accuracy of the present model Hamiltonian is particularly poor for OPW's which hybridize with the d states. Since these errors could arise from the assumed functional form for the radial form factors $f(k)$ and $g(k)$ in Eq. (9), we have compared the relative accuracy of several alternative forms. Since the overlap matrix element $\langle \vec{k} | d_n \rangle$ is simply the Fourier transform of the

TABLE III. Summary of energy-band states included in the nonlinear least-squares fitting procedure.

Type	Γ	X	L	W	K	Δ	Σ
OPW	Γ_1	X_1, X_4'	L_1, L_2'	W_1, W_3, W_2'	$2K_1, K_3$	Δ_1	Σ_1
					$2K_1, K_2$	Δ_1, Δ_2	$2\Sigma_1, \Sigma_2$
d	Γ_{12}, $\Gamma_{25'}$	X_1, X_2, X_3, X_5	$2L_3, L_1$	W_1, W_3, W_1', W_2'	K_3, K_4	Δ_2', Δ_5	Σ_3, Σ_4

tight-binding Bloch sum $|d_n\rangle$, then $f(k)$ in Eq. (5) corresponds to the radial part of the momentum wave function. If one assumes a hydrogenic form for ψ_n in Eqs. (2) and (3), then one can evaluate $f(k)$ directly (see Podolsky and Pauling[21]). It is found that little to no improvement in accuracy is achieved in the fit when these alternative forms are used. The reason is that, in the wave-vector range where hybridization is important [i.e., from $k=0$ to the first maximum in $f(k)$], the alternative forms for $f(k)$ exhibit the same k dependence as $j_2(kR)$.

Based on these studies, we conclude that the accuracy of the present model Hamiltonian is limited primarily by the size of the (4×4) plane-wave block. If a more accurate representation of the unoccupied states is required, then it will probably be necessary to add additional OPW's. By increasing the number of OPW's, one would also reduce the importance of the somewhat artificial symmetrizing factors in fitting the lowest conduction-band states.

APPENDIX: BLOCK DIAGONAL FORM OF MODEL HAMILTONIAN AT VARIOUS SYMMETRY POINTS

In the nonlinear least-squares fitting procedure used in Sec. IV, the parameters of the interpolation scheme were determined by fitting 40 levels of the first-principles calculations at the following seven points in the zone: $\Gamma(0,0,0)$, $X(0,8,0)$, $L(4,4,0)$, $W(4,8,0)$, $K(6,6,0)$, $\Delta(0,4,0)$, and $\Sigma(4,4,0)$. Each level was identified according to its group-theoretical transformation properties. We emphasize that the symmetrizing factors are essential if the Hamiltonian matrix is to be reduced to block diagonal form at points of high symmetry. Previously, some of these reduced matrices have been given in Sec. III. Here, we summarize the remaining results that have been used in the nonlinear least-squares fitting procedure. For the d-bands, we use the three-center nearest-neighbor approximation.

a. $\Gamma(0,0,0)$. We have

$$E(\Gamma_1) = V_{000}, \tag{A1}$$

$$E(\Gamma_{25'}) = E_0 - 4A_1 + 8A_2 \text{ (triply degenerate)}, \tag{A2}$$

$$E(\Gamma_{12}) = E_0 + \Delta + 4A_4 - 8A_5 \text{ (doubly degenerate)}, \tag{A3}$$

b. $X(0,8,0)$. We have

$$E(X_5) = E_0 + 4A_1, \tag{A4}$$

$$E(X_3) = E_0 - 4A_1 - 8A_2, \tag{A5}$$

$$E(X_2) = E_0 + \Delta + 4A_4 + 8A_5, \tag{A6}$$

c. $L(4,4,0)$. The block diagonal part of the Hamiltonian for the purely d-like L_3 levels is given by

$$H(L_3) = \begin{bmatrix} E_0 + 4A_3 & 4\sqrt{2}\,A_6 \\ 4\sqrt{2}\,A_6 & E_0 + \Delta \end{bmatrix}. \tag{A7}$$

Each solution is doubly degenerate.

d. $W(4,8,0)$. We have

$$E(W_1') = E_0 + 4A_1. \tag{A8}$$

e. $K(6,6,0)$. If we write

$$j_K = j_2(\sqrt{72}\,R), \tag{A9}$$

$$T = 72\alpha + V_{000} + S j_K^2, \tag{A10}$$

$$V'_{111} = V_{111} - \tfrac{1}{3} S j_K^2, \tag{A11}$$

$$V'_{200} = V_{200} + \tfrac{11}{27} S j_K^2, \tag{A12}$$

then we have

$$E(K_2) = E_0 + 2\sqrt{2}\,A_1 - 2A_2(\sqrt{2}-1) + 2A_3; \tag{A13}$$

$$E(K_4) = E_0 + \Delta + 2A_4 + 4\sqrt{2}\,A_5. \tag{A14}$$

The elements of the K_3 matrix are given by

$$H_{11} = T - V'_{200}, \tag{A15}$$

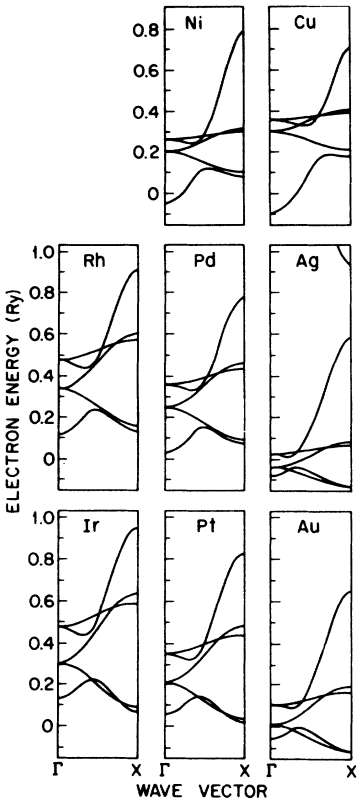

FIG. 4. Model band structures for the fcc d-band metals obtained by a nonlinear least-squares fit to nonrelativistic APW calculations.

TABLE IV. Parameters of the interpolation scheme obtained by a nonlinear least-squares fit to the results of nonrelativistic APW calculations on the fcc d-band metals.

	Ni	Cu	Rh	Pd	Ag	Ir	Pt	Au
α	0.0147	0.0138	0.0139	0.0130	0.0114	0.0142	0.0134	0.0121
V_{000}	−0.0517	−0.0904	0.1148	0.0310	−0.0797	0.1318	0.0534	−0.0497
V_{111}	0.0781	0.0613	0.0824	0.0701	0.0434	0.0687	0.0614	0.0437
V_{200}	0.1070	0.0921	0.0955	0.0894	0.0694	0.0932	0.0864	0.0728
R	0.4076	0.4073	0.4177	0.4104	0.4047	0.4212	0.4155	0.4094
S	0.7076	0.6761	1.5598	1.3056	0.8250	1.8966	1.6003	1.1743
B_t	1.0055	1.0085	1.5536	1.3429	0.8468	1.7373	1.5054	1.1176
B_e	1.0217	1.0202	1.5495	1.3381	0.9386	1.7163	1.5030	1.1609
E_O	0.2310	0.3302	0.4238	0.3136	−0.0005	0.4158	0.2998	0.0761
A_1	0.0200	0.0185	0.0448	0.0362	0.0210	0.0546	0.0448	0.0310
A_2	0.0056	0.0053	0.0112	0.0091	0.0054	0.0129	0.0107	0.0075
A_3	0.0076	0.0070	0.0154	0.0126	0.0074	0.0177	0.0148	0.0105
A_4	0.0110	0.0099	0.0238	0.0190	0.0102	0.0279	0.0226	0.0152
A_5	0.0027	0.0023	0.0061	0.0049	0.0029	0.0073	0.0060	0.0043
A_6	0.0093	0.0084	0.0213	0.0171	0.0095	0.0261	0.0212	0.0145
Δ	0.0022	0.0029	0.0001	0.0013	0.0041	0.0005	0.0017	0.0035
rms error	0.0035	0.0042	0.0130	0.0095	0.0041	0.0186	0.0137	0.0075
max error	0.0112	0.0125	0.0512	0.0371	0.0164	0.0767	0.0565	0.0307

$$H_{22} = E_0 + 2\sqrt{2} - 2A_2(\sqrt{2}-1) - 2A_3, \quad \text{(A16)}$$

$$H_{12} = \tfrac{4}{9} B_t j_K . \quad \text{(A17)}$$

The elements of the 4×4 K_1 matrix are

$$H_{11} = T, \quad H_{22} = T + V'_{200},$$

$$H_{33} = E_0 - 2A_1 - 4\sqrt{2}\,A_2,$$

$$H_{44} = E_0 + \Delta - \tfrac{2}{3}(A_4 + 4A_5) - \tfrac{4}{3}\sqrt{2}\,(2A_4 - A_5), \quad \text{(A18)}$$

$$H_{12} = \sqrt{2}\,V'_{111}, \quad H_{13} = \tfrac{1}{2} B_t j_K,$$

$$H_{14} = -\tfrac{1}{6}\sqrt{3}\,B_e j_K, \quad H_{23} = \tfrac{1}{18}\sqrt{2}\,B_t j_K,$$

$$H_{24} = \tfrac{5}{18}\sqrt{6}\,B_e j_K, \quad H_{34} = -(4/\sqrt{3})\,A_6 .$$

f. $\Delta(0, 4, 0)$. Let us write

$$T_1 = 16\alpha + V_{000} + S[j_2(\sqrt{16}\,R)]^2, \quad \text{(A19)}$$

$$T_2 = 144\alpha + V_{000} + S[j_2(\sqrt{144}\,R)]^2, \quad \text{(A20)}$$

$$V'_{200} = V_{200} + S j_2(\sqrt{16}\,R)\, j_2(\sqrt{144}\,R), \quad \text{(A21)}$$

$$F_\Delta = F_2 = \sin^{1/2}\tfrac{1}{6}\pi = 2^{-1/2} . \quad \text{(A22)}$$

TABLE V. Alternative set of parameters for the interpolation scheme using, for the d bands, a two-center approximation taken to second nearest neighbors.

	Ni	Cu	Rh	Pd	Ag	Ir	Pt	Au
α	0.0147	0.0139	0.0138	0.0130	0.0114	0.0142	0.0134	0.0121
V_{000}	−0.0529	−0.0917	0.1169	0.0310	−0.0787	0.1351	0.0555	−0.0487
V_{111}	0.0766	0.0597	0.0820	0.0690	0.0422	0.0690	0.0608	0.0425
V_{200}	0.1093	0.0949	0.0976	0.0119	0.0715	0.0944	0.0883	0.0752
R	0.4113	0.4093	0.4159	0.4099	0.4069	0.4189	0.4140	0.4099
S	0.7070	0.6824	1.5294	1.2874	0.8463	1.8639	1.5803	1.1801
B_t	1.0134	1.0162	1.5924	1.3726	0.8309	1.7745	1.5368	1.1270
B_e	0.9765	0.9685	1.5547	1.3239	0.8583	1.7352	1.4993	1.1114
E_o	0.2303	0.3292	0.4240	0.3135	−0.0025	0.4149	0.2990	0.0745
$(dd\sigma)_1$	−0.0260	−0.0242	−0.0589	−0.0474	−0.0272	−0.0718	−0.0587	−0.0405
$(dd\pi)_1$	0.0121	0.0111	0.0243	0.0199	0.0117	0.0281	0.0233	0.0165
$(dd\delta)_1$	−0.0014	−0.0009	−0.0027	−0.0022	−0.0016	−0.0027	−0.0024	−0.0019
$(dd\sigma)_2$	−0.0008	−0.0008	0.0019	0.0009	0.0002	0.0029	0.0018	0.0004
$(dd\pi)_2$	0.0004	0.0005	0.0007	0.0006	0.0011	0.0014	0.0012	0.0011
$(dd\delta)_2$	−0.0000	−0.0003	−0.0003	−0.0001	−0.0001	−0.0005	−0.0003	−0.0002
Δ	0.0021	0.0035	−0.0010	0.0002	0.0041	0.0008	0.0014	0.0034
rms error	0.0039	0.0045	0.0131	0.0097	0.0045	0.0185	0.0137	0.0077
max error	0.0116	0.0132	0.0518	0.0378	0.0172	0.0772	0.0573	0.0316
$(dd\pi)_1/(dd\sigma)_1$	0.466	0.459	0.413	0.420	0.430	0.393	0.398	0.408

The elements of the 3×3 Δ_1 matrix are the following:

$$H_{11}=T_1,\quad H_{22}=T_2,$$
$$H_{33}=E_0+\Delta-\tfrac{4}{3}(4A_5+A_4),\quad H_{12}=V'_{200}F_\Delta,$$
$$H_{13}=-(1/\sqrt{3})B_e j_2(\sqrt{16}R),$$
$$H_{23}=-(1/\sqrt{3})B_e j_2(\sqrt{144}R)F_\Delta. \tag{A23}$$

For the other symmetries, we have

$$E(\Delta_5)=E_0+4A_2 \quad \text{(doubly degenerate)}, \tag{A24}$$
$$E(\Delta_{2'})=E_0-4A_1, \tag{A25}$$
$$E(\Delta_2)=E_0+\Delta+4A_4. \tag{A26}$$

g. $\Sigma(4,4,0)$. Let us write

$$T_1=32\alpha+V_{000}+S[j_2(\sqrt{32}R)]^2, \tag{A27}$$
$$T_2=96\alpha+V_{000}+S[j_2(\sqrt{96}R)]^2, \tag{A28}$$
$$V'_{111}=V_{111}, \tag{A29}$$
$$V'_{200}=V_{200}-\tfrac{1}{3}S[j_2(\sqrt{96}R)]^2, \tag{A30}$$
$$F_\Sigma=F_3=F_4=\sin^{1/2}\tfrac{1}{4}\pi=2^{-1/4}. \tag{A31}$$

The elements of the 4×4 Σ_1 matrix are

$$H_{11}=T_1,\quad H_{22}=T_2+V'_{200}F_\Sigma^2,$$
$$H_{33}=E_0,\quad H_{44}=E_0+\Delta,$$
$$H_{12}=\sqrt{2}\,V'_{111}F_\Sigma,\quad H_{13}=\tfrac{1}{2}B_t j_2(\sqrt{32}R),$$
$$H_{14}=-\tfrac{1}{6}\sqrt{3}B_e j_2(\sqrt{32}R),\quad H_{23}=\tfrac{1}{6}\sqrt{2}B_t j_2(\sqrt{96}R)F_\Sigma,$$
$$H_{24}=(1/\sqrt{6})B_e j_2(\sqrt{96}R)F_\Sigma,\quad H_{34}=-(8/\sqrt{3})A_6. \tag{A32}$$

The corresponding results for the 2×2 Σ_3 matrix are

$$H_{11}=T_2-V'_{200}F_\Sigma^2,\quad H_{22}=E_0-4A_3,$$
$$H_{12}=\tfrac{2}{3}B_t j_2(\sqrt{96}R)F_\Sigma. \tag{A33}$$

For the remaining states, we have

$$E(\Sigma_2)=E_0+4A_3, \tag{A34}$$
$$E(\Sigma_4)=E_0+\Delta. \tag{A35}$$

[1]N. V. Smith, Phys. Rev. B 3, 1862 (1971).
[2]N. V. Smith, Phys. Rev. B 5, 1192 (1972).
[3]L. Hodges, H. Ehrenreich, and N. D. Lang, Phys. Rev. 152, 505 (1966); H. Ehrenreich and L. Hodges, in *Methods in Computational Physics*, edited by B. Alder, S. Fernbach, and M. Rotenberg (Academic, New York, 1968), Vol. 8, p. 149.
[4]F. M. Mueller, Phys. Rev. 153, 659 (1967).
[5]J. C. Slater and G. F. Koster, Phys. Rev. 94, 1498 (1954).
[6]G. C. Fletcher and E. P. Wohlfarth, Philos. Mag. 42, 106 (1951).
[7]G. C. Fletcher, Proc. Phys. Soc. Lond. A 65, 192 (1952).
[8]J. C. Slater, Phys. Rev. 45, 794 (1937); J. M. Ziman, in *Solid State Physics*, edited by H. Ehrenreich, F. Seitz, and D. Turnbull (Academic, New York, 1971). Vol. 26, p. 1.
[9]The units in which wave vectors are expressed are such that the distance from Γ to X is 8.
[10]G. A. Burdick, Phys. Rev. 129, 138 (1963).
[11]L. Hodges, Ph.D. thesis (Harvard University, 1966) (unpublished).
[12]V. Heine, Phys. Rev. 153, 673 (1967).
[13]J. Friedel, P. Lenglart, and G. Leman, J. Phys. Chem. Solids 25, 781 (1964); E. Abate and M. Asdente, Phys. Rev. 140, A1303 (1965).
[14]F. Herman and S. Skillman, *Atomic Structure Calculations* (Prentice-Hall, Englewood Cliffs, N.J., 1963).
[15]N. E. Christensen and B. O. Seraphin, Phys. Rev. B 4, 3321 (1971).
[16]J. C. Slater, Phys. Rev. 81, 385 (1951).
[17]L. F. Mattheiss, Phys. Rev. 181, 987 (1969).
[18]D. D. Koelling, A. J. Freeman, and F. M. Mueller, Phys. Rev. B 1, 1318 (1970).
[19]O. K. Andersen, Phys. Rev. B 2 883 (1970).
[20]L. F. Mattheiss, Phys. Rev. B 5, 290 (1972).
[21]B. Podolsky and L. Pauling, Phys. Rev. 34, 109 (1929).